Journal of Geochemical Exploration 278 (2025) 107860

Contents lists available at ScienceDirect

Journal of Geochemical Exploration

journal homepage: www.elsevier.com/locate/gexplo

Improving the performance of contamination indices by accounting for local baselines in stream sediment: A sample catchment basin approach

Iannone Antonio, Dominech Salvatore *, Pacifico Lucia Rita, Guarino Annalise, Albanese Stefano

Department of Earth Sciences, Environment and Resources (DiSTAR), University of Naples Federico II, 80126 Naples, Italy

ARTICLE INFO

Keywords:
Pollution indices
Local baselines
Regional baselines
Sensitivity analysis
Enrichment factor
Contamination factor

ABSTRACT

Geochemical prospecting serves as a fundamental approach for examining the influence of geological settings on stream sediment composition and identifying natural or anthropogenic geochemical anomalies within a river catchment. Various indices have been developed to assess sediment quality and environmental status, typically based on ratios between observed element concentrations and reference values representing undisturbed conditions. However, these reference values often fail to account for the influence of river dynamics on sediment variability, potentially compromising the reliability of contamination assessments. Since the chemical composition of stream sediments reflects the cumulative influence of their upstream catchment basins, the dilution correction method has been extensively employed in previous studies to mitigate the dilution effects caused by fluvial processes. To address this, the present study evaluates whether local geochemical baselines can improve the performance of contamination indices. The Sarno River basin, heavily impacted by urban and industrial activities, was selected as a case study. Ninety-six sediment samples were analysed using geomorphological and hydrological parameters to define each Sample Catchment Basin (SCB). Baseline concentrations of Cd, Cr, Cu, Hg, Ni, Pb, Sb, and Zn were then estimated by calculating the weighted average element content based on lithological unit proportions within each SCB. Then, contamination indices were computed using both uncorrected (raw) and SCB-corrected baselines and spatially mapped. The use of SCB-based reference values led to a 23 % increase in the detection of high-impact sites using the Enrichment Factor and a 366 % increase using the Contamination Factor, revealing a substantial underestimation of contamination in the raw approach. Comparative analysis also showed a more balanced distribution of element contributions in the corrected indices, indicating improved representativeness of multi-element contamination. These results highlight the advantages of incorporating local baseline variability into geochemical evaluations, providing a more accurate and spatially consistent framework for environmental risk assessment in fluvial systems.

1. Introduction

In a river context, several natural and anthropogenic factors contribute to the chemical composition of stream sediments along the river path from the headwaters to the mouth. Among the natural factors, lithology, topography, and drainage density all influence the chemical composition of stream sediments by affecting the availability of minerals and contaminants, the rate of erosion and sediment transport, and the spatial distribution of sediment sources within a watershed. Anthropogenic factors can also significantly contribute to the chemical composition of stream sediments; they include: i) mechanical factors, such as deviations and infrastructures, which can alter erosion rates and the distribution of pollutants in the watersheds; ii) chemical factors, such as urbanization, industrial activities, agricultural practices which contribute to introduce directly various chemicals and potentially toxic elements (PTEs) in the environment, impacting the quality of stream sediments, aquatic ecosystems, and the overall integrity of freshwater resources (Ip et al., 2005; Luo et al., 2024). Additionally, river dynamics have become more complicated due to ongoing climate change, which affects the frequency and intensity of flooding phenomena and polluted stormwater runoff (Johnson et al., 2022).

In the last decades, a wide variety of tools have been developed to assess the chemical contamination of sediments. These include the contamination indices, a broadly used method to evaluate the overall

* Corresponding author.
E-mail address: salvatore.dominech@unina.it (D. Salvatore).

https://doi.org/10.1016/j.gexplo.2025.107860
Received 28 February 2025; Received in revised form 17 June 2025; Accepted 1 July 2025
Available online 5 July 2025

environmental quality in various ecosystems. Contamination indices are generally divided into individual and complex indices; the former assesses overall pollution relative to a single element, while the latter allows for the determination of overall pollution relative to a group of elements. Among the individuals, the most widely used are the Contamination Factor (CF) (Hakanson, 1980), the Enrichment Factor (EF) (Ergin et al., 1991), and the Geo-accumulation Index (I_{geo}) (Muller, 1969). Among the complex indices, there are the Contamination Degree (CD) (Hakanson, 1980), the Cumulative Contamination Index (CCI) (Aruta et al., 2023), Contamination Severity Index (CSI) (Pejman et al., 2015), Pollution Load Index (PLI) (Tomlinson et al., 1980), Nemerow Pollution Index ($PI_{Nemerow}$) (Cheng et al., 2007), and others. However, it is well known that the calculation of pollution indices in soils and sediments is based on an accurate definition of the geochemical reference levels, typically distinguished in geochemical background and baseline. The first refers to the natural concentration, unaffected by human influence; in contrast, the baseline refers to the concentration content in a specific area and at a particular time, which includes both the natural background and a minor contribution from diffuse, long-term anthropogenic contamination. Selecting appropriate reference values is crucial for accurately assessing pollution levels in environmental matrices, avoiding under- or overestimation. In many studies, global reference values, such as the average content in the upper continental crust, are adopted (Kalita et al., 2019; Varol et al., 2020; Wang et al., 2025) but this provides a generalized baselines that may ignore local geological variability.

Many recent studies also emphasized the use of regional reference values as more appropriate for contamination assessment. Such values better reflect the natural geological variability of an area compared to the global background concentration (Carrillo et al., 2021; Kowalska et al., 2018; Niu et al., 2024; Wang et al., 2019). Standard statistical-based methods used to establish regional reference values include the Cumulative Frequency Method, Mean + 2σ (Matschullat et al., 2000; Reimann et al., 2005), the iterative 2σ- and 4σ-outlier techniques (Matschullat et al., 2000), the Upper Tolerance Limit. However, none of these methods take into account the geolithological variability that occurs within a single catchment basin at a local scale. Thus, the performance of a contamination index, which is deeply influenced by the assessment of a reference value, may lead to misinterpretation of the contamination levels from one site to another, even within the same river catchment. Additionally, most aggregate indices are based on a linear aggregation function, such as the sum of individual indices; they implicitly assume that the individual indicator's influence on the aggregate indicator's value remains constant, regardless of its value. Based on the previous considerations, this work aimed to improve the performance of two widely used indices, taking into account the variability of the geochemical background/baseline values in relation to the geolithological heterogeneity of the substrate and the dynamic nature of the transported sediment.

The Sarno River basin was chosen as a case study since it has been recognized as one of the most polluted in Europe (Montuori et al., 2015; Pepi et al., 2016). As reported by Montuori et al. (2013), the Sarno exhibited higher concentration of several elements, such as Hg, Cr, Zn, Cd, Pb, when compared to several other rivers, including the Seyhan River (Turkey), Gediz River (Aegean), Tigris River (Turkey), Ebro River (Spain), and Po River (Italy). Even regarding organophosphate pesticides, the Sarno showed generally higher levels compared to those measured in the Arc River (France), the Huveaune River (France), and the Guan River (China). Additionally, it is not free of climatic variation and associated flooding events; in fact, it has historically been the site of numerous hazardous hydrogeological events, including flash floods and landslides (Califano et al., 2015; Longobardi et al., 2016). Its vulnerability to urban flooding is notably high because of its population of more than one million residents. This makes the Sarno River Basin one of Italy's most densely populated areas, highly vulnerable to both anthropogenic pollution and extreme hydrogeological events, making it an excellent candidate for our purpose.

2. Study area

The Sarno River Basin (approximately 500 km^2), encompassing the alluvial plain of the Sarno River and the basins of its tributaries, Solofrana and Cavaiola, is located in the Campania region in southern Italy. It is bordered by the volcanic complex of Somma-Vesuvio on the northwest, the Sarno Mountains on the northeast, the Lattari Mountains on the south, the Tyrrhenian Sea on the west, and the Picentini Mountains on the east (Fig. 1). Originating at the base of limestone formations within the Apennine Chain, the headwaters of the Sarno River sustain a daily average flow of approximately 1 $m^3 \cdot s^{-1}$, coursing through a path of 24 km across the agricultural lands of San Marzano and Scafati before discharging into the Tyrrhenian Sea (Arienzo et al., 2001).

The Sarno River basin is characterised by a Mediterranean climate. Its average annual temperature is 17.2 °C, and its average annual rainfall is about 1203 mm, with precipitation mainly concentrated in the autumn-winter seasons (Ufficio Idrografico e Mareografico di Napoli, 1960–1995). Geologically, the Sarno River Basin (Fig. 1a) is primarily made up of carbonates belonging to the Campano-Lucanian and Abruzzese-Campanian platforms across the Sarno and Picentini Mountains (Fig. 1a). These formations include Triassic dolomite, dolomitic limestone of the lower Jurassic-Cretaceous period, and fractured, karstified limestone from the Cretaceous era (De Pippo et al., 2006). Additionally, pyroclastic deposits and volcanic ash related to the activity of Mount Somma-Vesuvius predominantly overlay the calcareous-dolomitic rock of the Sarno Mountains, as well as the Sarno River plain (Cinque et al., 1997). Several hazardous hydrogeological events, including flash floods and landslides, have affected the basin in the last decades (Califano et al., 2015; Longobardi et al., 2016). The basin also represents a significant associated vulnerability, being one of the most densely populated areas in southern Italy (>1 million people and an average population density of about 1800 inhabitants per km^2).

According to the classification provided by the Corine Land Cover project (EEA, 2018) (Fig. 1b), much of the coastal and inland areas within the basin have undergone significant urbanization and industrialisation, with a massive presence of leather tannery plants in the upper valley, spanning from Solofra to Mercato S. Severino and Fisciano (Arienzo et al., 2001). In the middle part of the Sarno basin, intensive agricultural practices (horticulture, orchards, vineyards, chestnut groves, and greenhouse horticulture and floriculture) are predominant (Fig. 1b), thanks to the remarkable fertility of the soil given by physical and chemical interactions with pyroclastic deposits (Rolandi et al., 2008). Conversely, the economy of the lower Sarno Valley is characterised by the presence of various chemical-pharmaceutical, engineering, and manufacturing industries (De Pippo et al., 2006).

3. Material and methods

3.1. Sample treatment and chemical analysis

The 97 samples falling within the Sarno River basin were selected from a broader geochemical dataset that covers the entire regional territory. All laboratory analyses were conducted within a single analytical batch across the full regional dataset, from which the geochemical data related to the Sarno basin were subsequently extracted. Sampling was performed at an average sampling density of one sample per 5 km^2. Each sample was collected at the centre of the streams (avoiding the collection of organic matter), mixing sample materials from five different spots along a stream stretch of 200–500 m. After collecting, the samples were treated at the Environmental Geochemistry Laboratory of the Department of Earth, Environmental and Resources Sciences (University of Naples Federico II). The samples were dried and sieved, collecting 30 g of the fraction <150 μm.

A total of 37 elements (Ag, Al, As, Au, B, Ba, Bi, Ca, Cd, Co, Cr, Cu, Fe,

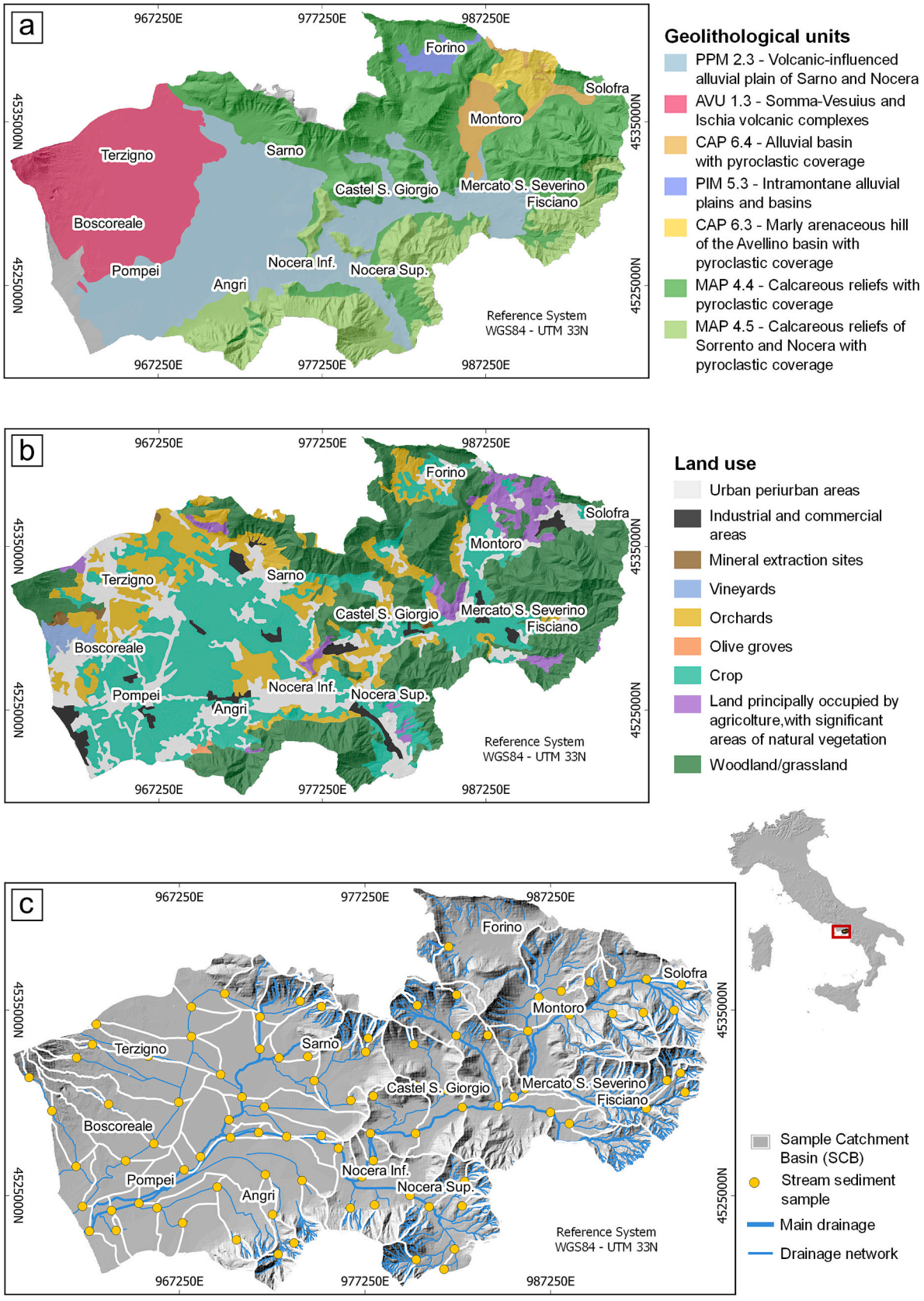

Fig. 1. Study area characterization. (a) Geolithological map showing the distribution of volcanic, alluvial, marly, and calcareous units within the Sarno River Basin. (b) Land use classification across the SCBs, highlighting urban, industrial, agricultural, and natural vegetation areas (EEA, 2018). (c) Drainage network and sampling points within the Sample Catchment Basins. All maps use the WGS84 UTM Zone 33 N coordinate reference system.

Ga, Hg, K, La, Mg, Mn, Mo, Na, Ni, P, Pb, S, Sb, Sc, Se, Sr, Te, Th, Ti, Tl, U, V, W and Zn) were analysed at Acme Analytical Laboratories Ltd. (Vancouver, Canada) using Inductively Coupled Plasma Mass Spectrometry (ICP-MS) and Inductively Coupled Plasma Optical Emission Spectroscopy (ICP-OES). Specifically, a 15-gram split of the pulp was digested in a 45 mL mixture of aqua regia at 90 °C for 1 h. The resulting solution was then brought to a final volume of 300 mL with 5 % HCl. Aliquots of the sample solution were aspirated into a Jarrel Ash Atomcomp 975 ICP-Emission Spectrometer and a Perkin Elmer Elan 6000 ICP-Mass Spectrometer for analysis. The Aqua Regia leaching represents an extraction method capable of dissolving various minerals, including sulphides, carbonates, clay minerals, as well as primary and secondary salts and hydroxides and, partially, some select silicates such as olivine and trioctahedral micas (Salminen, 1995).

For this study, only a selected group of elements was examined: Cd, Cr, Cu, Hg, Ni, Pb, Sb, and Zn. These PTEs were chosen based on their relevance as anthropogenic contaminants in the area, as confirmed by previous multivariate geochemical analyses (Albanese et al., 2013). In particular, these elements are commonly associated with primary sources of contamination such as tanneries, vehicular traffic, and agricultural fertilisers.

To enhance analytical accuracy and improve correction of spectral interferences, sample solutions were examined using both ICP-MS and ICP-OES techniques. This dual-method approach also increases the measurable range for key major elements such as Ca, Fe, and P. Calibration of the instruments was performed using a sequence of 40 calibration standards applied at the start and end of each analytical batch. To ensure reliable internal standardization, a tracer element was introduced directly into the digestion solution (spiked solution). Measurement precision at detection limits was estimated to be approximately ±100 %, but this improved significantly, surpassing ±10 %, once concentrations reached 50 times the detection threshold. These precision values were derived from triplicate in-house tests and blind duplicate samples. Accuracy was determined using a proprietary reference standard (DS2) developed by Acme Laboratories. DS2 was calibrated via ICP-MS following an aqua regia digestion, with validation against published concentrations from Canadian Certified Reference Materials (CCRMP), specifically TILL-4 and LKSD-2, which were digested using concentrated HCl and HNO_3. Procedural and analytical blanks were also measured, consistently showing very low concentrations, confirming the reliability of the analytical results. Table 1 reports the main statistical parameters, detection limits, and accuracy and precision values.

3.2. Baseline estimation

Two distinct methodologies were employed and compared to determine the most precise approach for establishing the geochemical baseline. The first method used a classical approach commonly employed in geochemical studies to calculate a unique baseline value for the study area: the Upper Regional Baseline Limit (URBL).

However, recognising the inherent geochemical variability within the study area, a more refined approach has also been employed by calculating Local Baselines (LBs) within the study area. This involved the use of the SCB approach, wherein weighted mean concentration values were calculated for each element within each sample catchment, obtaining more precise baseline values. The following section presents both methods. Boxplots comparing LBs and URBL values have been generated to evaluate the difference between the two approaches (SM1).

3.2.1. Upper regional baseline limit (URBL)

Since geochemical data are usually positively skewed, it is advisable to transform elemental concentrations showing an asymmetric empirical density distribution before proceeding with any further analysis (Carranza, 2011, 2009). Therefore, the data distribution's symmetry was improved through a log transformation. Subsequently, boxplots with log-transformed data were generated for each element to identify outliers, which were then excluded from further analysis to minimise their influence and ensure the accuracy of the baseline assessment. Nine samples were identified as outliers for Cr; five for Cu; two for Hg, Sb, and Zn; seven for Hg; and one for Pb and Cd.

The baseline levels of each of the eight variables considered were determined using ProUCL 5.2 software, which calculated the 95 % Upper Tolerance Limit (UTL) with 95 % coverage based on the dataset's distribution type (e.g., normal, log-normal, gamma, non-parametric). Then, the resulting UTL values were back-transformed to obtain the raw concentration value.

3.2.2. Local baselines (LBs)

The total catchment area was divided into Sample Catchment Basins (SCBs) (Fig. 1c), each representing the upstream and upslope region contributing to a specific sampling site, extending to the next sampling point and bounded by the drainage divides (Bonham-Carter et al., 1987b; Carranza and Hale, 1997). More generally, a Stream Catchment Basin (SCB) refers to a section of the catchment defined mainly by its geomorphological and hydrological features, encompassing the area that directly affects the geochemical makeup of the downstream sample collected at its outlet (Lancianese and Dinelli, 2015). A Sample Catchment Basin (SCB) analysis has been conducted in a GIS environment using the geomorphological and hydrological features of a digital elevation model (DEM) with a 10 m resolution (Tarquini et al., 2023).

There are two feasible options for the delineation of the zone of influence: i) considering all the upstream area until the surface watershed (Najafian et al., 2020); ii) considering all the upstream area until the following stream sediment sample (Dominech et al., 2022; Habibnia et al., 2019). The second option has been preferred because it enhances the process closest to the sample rather than the distal ones. Subsequently, according to (Bonham-Carter et al., 1987a), the weighted mean uni-element concentration (M_j) was calculated for each *j-th* lithologic unit (j = 1, 2, …, m) in the *i-th* sample catchment basin (SCB_i) (*i* = 1, 2, …, n) through the application of the following equation (Eq. (1)):

Table 1
Univariate statistics for selected elements together with detection limits (DLs), accuracy (ACC), and precision (RPD).

Element	Unit	DLs	Min	Max	Mean	Median	SD	MAD	CVR (%)	Skewness	Kurtosis	RPD (%)	ACC (%)
Cd	mg/kg	0.01	0.08	1.18	0.38	0.33	0.20	0.18	53.9	1.09	1.72	1.4	5.6
Cr	mg/kg	0.5	5.40	1117	65.9	14.3	172	8.90	62.2	4.93	26.9	3.2	1.5
Cu	mg/kg	0.01	17.3	1335	142	87	197	56	64.4	4.06	18.3	3.7	1.6
Hg	µg/kg	5	3.80	1156	142	72	202	57.8	80.3	3.13	10.9	8.0	0
Ni	mg/kg	0.1	6.50	43.5	16.6	15.6	5.50	2.97	19	1.94	6.20	1.7	0.6
Pb	mg/kg	0.01	19.3	228	68.4	55.8	37.9	20.7	37	1.72	3.31	3.5	0.6
Sb	mg/kg	0.02	0.28	4.86	0.86	0.65	0.68	0.30	45.6	3.32	14.5	3.1	1.2
Zn	mg/kg	0.1	38.9	511	144	110	101	50.7	46.1	1.88	3.09	2.6	0.5
Fe	%	0.01	1.14	10.9	2.64	2.62	0.61	0.61	23.2	0.12	0.20	1.3	0.7

Where: SD means Standard Deviation, MAD means Median Absolute Deviation, CVR means robust coefficient of variation.

$$Mj = \frac{\sum_{i=1}^{n} Y_i X_{ij}}{\sum_{i=1}^{n} X_{ij}} \quad (1)$$

where Y_i is the concentration value (raw) of the element in the stream sediment sample i (= 1, 2, …, n) and X_{ij} is the area of each lithologic unit j (= 1, 2, …, m) in each SCB.

In the classical SCB approach, X_{ij} represents the 2D area of the surface and not the three-dimensional one. However, the areal proportion can significantly differ if we consider the actual 3D surface instead of its projection on the plane. The calculation of the 3D area for each lithological unit involved several computational steps. Initially, the slope for every pixel within the DEM was calculated in the QGIS environment using the Geospatial Data Abstraction Library (GDAL) plugin; subsequently, the cosine of the slope was determined for each pixel. Then, starting from the principles of trigonometry (Eq. (2)) and knowing the cosine of the slope and the basal area of the triangle (base cathetus), for each pixel, the area of the hypotenuse (the actual surface) was derived via Eq. (3):

$$\cos\theta = \frac{cathetus\ area}{hypotenuse\ area} \quad (2)$$

$$Hypotenuse\ area = \frac{Cathetus\ area}{\cos\theta} \quad (3)$$

Then, the sum of the 3D area for all pixels associated with a particular lithological unit is computed through the statistical zoning plugin in the QGIS environment. Therefore, this study determines the 3D area of each lithological unit, ensuring a comprehensive consideration of geomorphological characteristics in the SCB method. Following the calculation of the weighted value Mj, the local uni-elemental background/baseline values, hereafter Local Baselines (LBs), were calculated for each SCB according to the Eq. (4):

$$LB = \frac{\sum_{j=1}^{m} M_j X_{ij}}{\sum_{j=1}^{m} X_{ij}} \quad (4)$$

3.3. Assessment of the Pollution Indices

For this study, two individual indices, Contamination Factor (CF) and Enrichment Factor (EF), and their corresponding aggregate functions, Cumulative Contamination Index (CCI) and Contamination Degree (CD), were chosen to evaluate contamination. These two indices were selected due to their simple application, which makes them easily replicable and widely utilised in the literature (Barbieri, 2016; Haris et al., 2017; He et al., 2019; Loska et al., 1997). This simplicity also facilitates comparisons with other similar case studies.

The CF provides a straightforward assessment of contamination levels by dividing the concentrations of target elements by a reference value, typically derived from background/baseline or uncontaminated sites (Eq. (5)):

$$CF = \frac{C_{heavy\ metal}}{C_{reference}} \quad (5)$$

The EF evaluates the enrichment of specific elements compared to a reference element which is abundant and present in the sediment in a relatively constant proportion, to measure the possible impact of anthropogenic activity on the concentration of PTEs (Eq. (6)):

$$EF = \frac{\left[\frac{C_n}{C_{ref}}\right] sample}{\left[\frac{B_n}{B_{ref}}\right] baseline} \quad (6)$$

where:

$\left[\frac{C_n}{C_{ref}}\right]$ sample – ratio of the analysed PTE and the concentration of the reference element;

$\left[\frac{B_n}{B_{ref}}\right]$ baseline – ratio of the background value of the analysed PTE and the baseline of the reference element.

In Eq. (6), Fe was chosen as the reference element for several reasons: i) because of its low Robust Coefficient Variation (CVR) (Reimann et al., 2008) (Table 1); ii) for its high abundance in Earth's crust; iii) it is generally associated to the finest grain size (Kadhum et al., 2015; Varol, 2011), which aligns with the fraction we used for the chemical analyses, allowing us to deduce with high confidence that its values are not being underestimated.

The Contamination Degree (CD) represents the aggregate function of the CF; it is defined as the sum of all contamination factors, according to the Eq. (7):

$$CD = \sum_{i=1}^{n} CF_i \quad (7)$$

where CF_i is the single contamination factor, and n is the number of considered elements.

The Cumulative Contamination Index (CCI) corresponds to the aggregate function of the Enrichment Factor, and it is defined as the sum of all the EFs, according to Eq. (8):

$$CCI = \sum_{i=1}^{n} EF_i \quad (8)$$

where EF_i is the single enrichment factor, and n is the number of elements considered.

The URBL value was used as the baseline value for each element in raw data. For SCB-corrected data, a local baseline value was assigned to each SCB and used to calculate the CFs and EFs values (Eqs. (5) and (6)) and, consequently, the corresponding aggregate functions, CD (Eq. (7)) and CCI (Eq. (8)).

Geochemical mapping was performed to illustrate the spatial variability of local baselines (Fig. 2) and contamination indices (Figs. 3, 4, 5, 6, 7). For local baseline values, probability plots (P-plots) were used as a classification method to identify breakpoints along the curve. For CFs, maps were classified according to Hakanson (1980) as follows:

- $CF < 1$ No/low contamination.
- $1 \leq CF \leq 3$ Moderate contamination.
- $3 \leq CF \leq 6$ Considerable contamination.
- $CF > 6$ Very high contamination.

For EFs, maps were classified into five categories as follows (Vineethkumar et al., 2020):

- $EF < 1$ No enrichment
- $1 \leq EF \leq 2$ Minimal enrichment.
- $2 \leq EF \leq 5$ Moderate enrichment.
- $5 \leq EF \leq 20$ Significant enrichment.
- $EF > 20$ Very high enrichment.

Otherwise, for the geochemical mapping of the aggregate function CD and CCI, values were reclassified considering the classification proposed by Hakanson (1980) and Vineethkumar et al. (2020), as well as the number of potentially toxic elements (7) considered in this study.

For CD, values were reclassified as follows:

- $CD < 7$ No contamination.
- $7 \leq CD \leq 14$ Moderate contamination.
- $14 \leq CD \leq 28$ High degree of contamination.

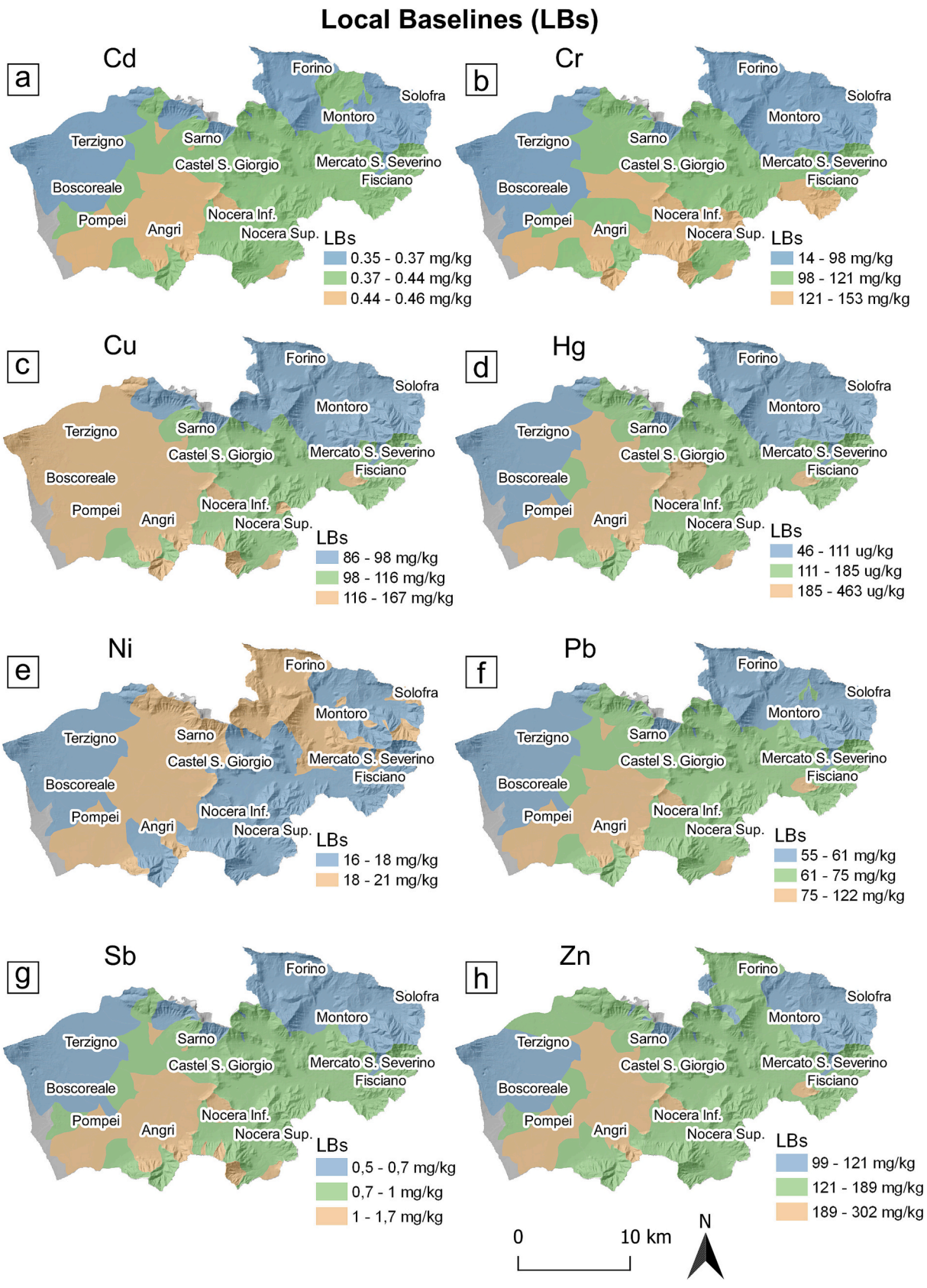

Fig. 2. Spatial distribution of local baseline (LB) concentrations for potentially toxic elements (PTEs) in stream sediment samples across the study area. Maps show LB values for (a) cadmium (Cd), (b) chromium (Cr), (c) copper (Cu), (d) mercury (Hg), (e) nickel (Ni), (f) lead (Pb), (g) antimony (Sb), and (h) zinc (Zn). Concentration ranges are expressed in mg/kg for all elements except Hg, which is in μg/kg.

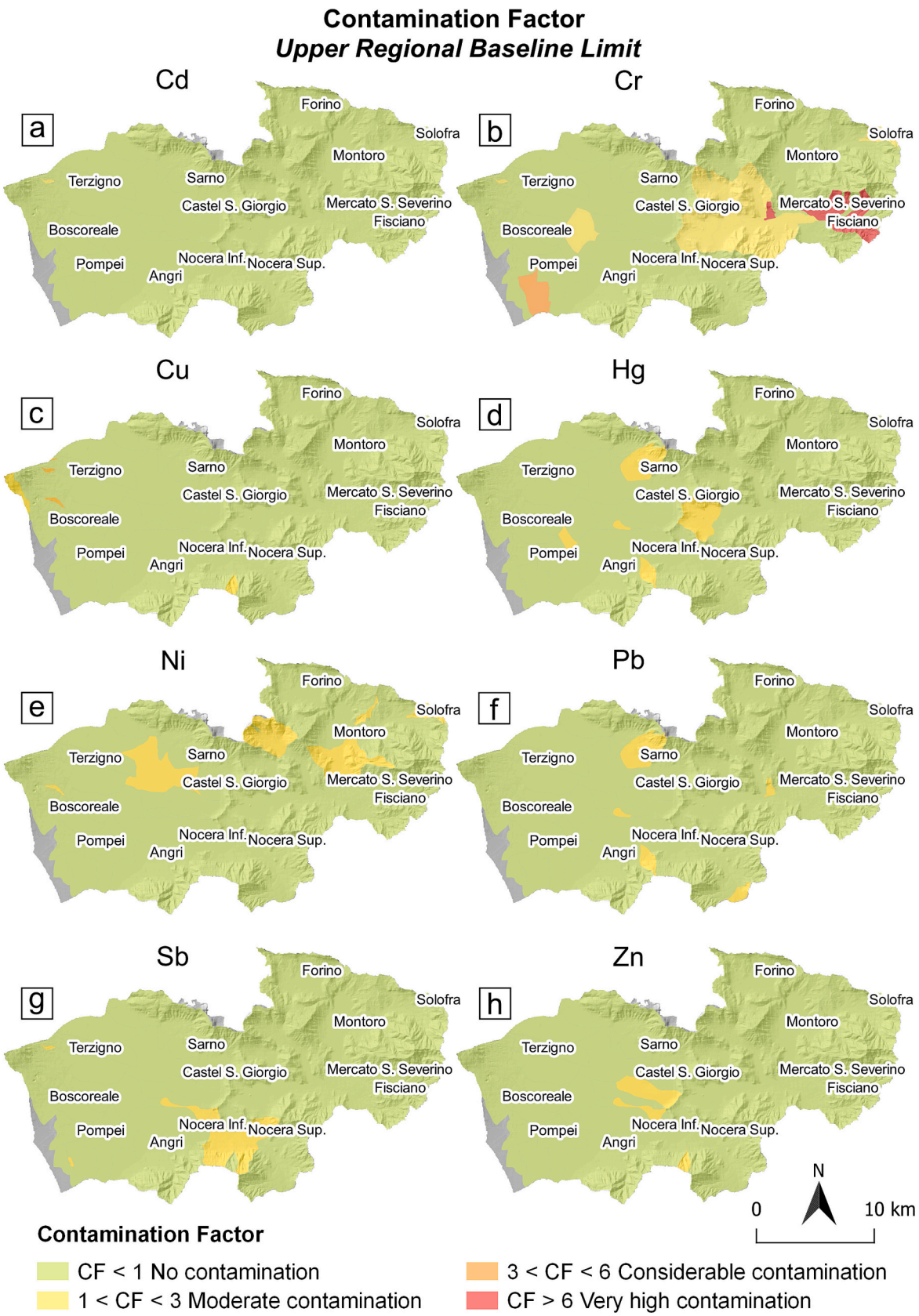

Fig. 3. Contamination Factor -Upper Regional Baseline Limit (URBL) distribution maps for a) cadmium, b) chromium, c) copper, d) mercury, e) nickel, f) lead, g) antimony, h) zinc.

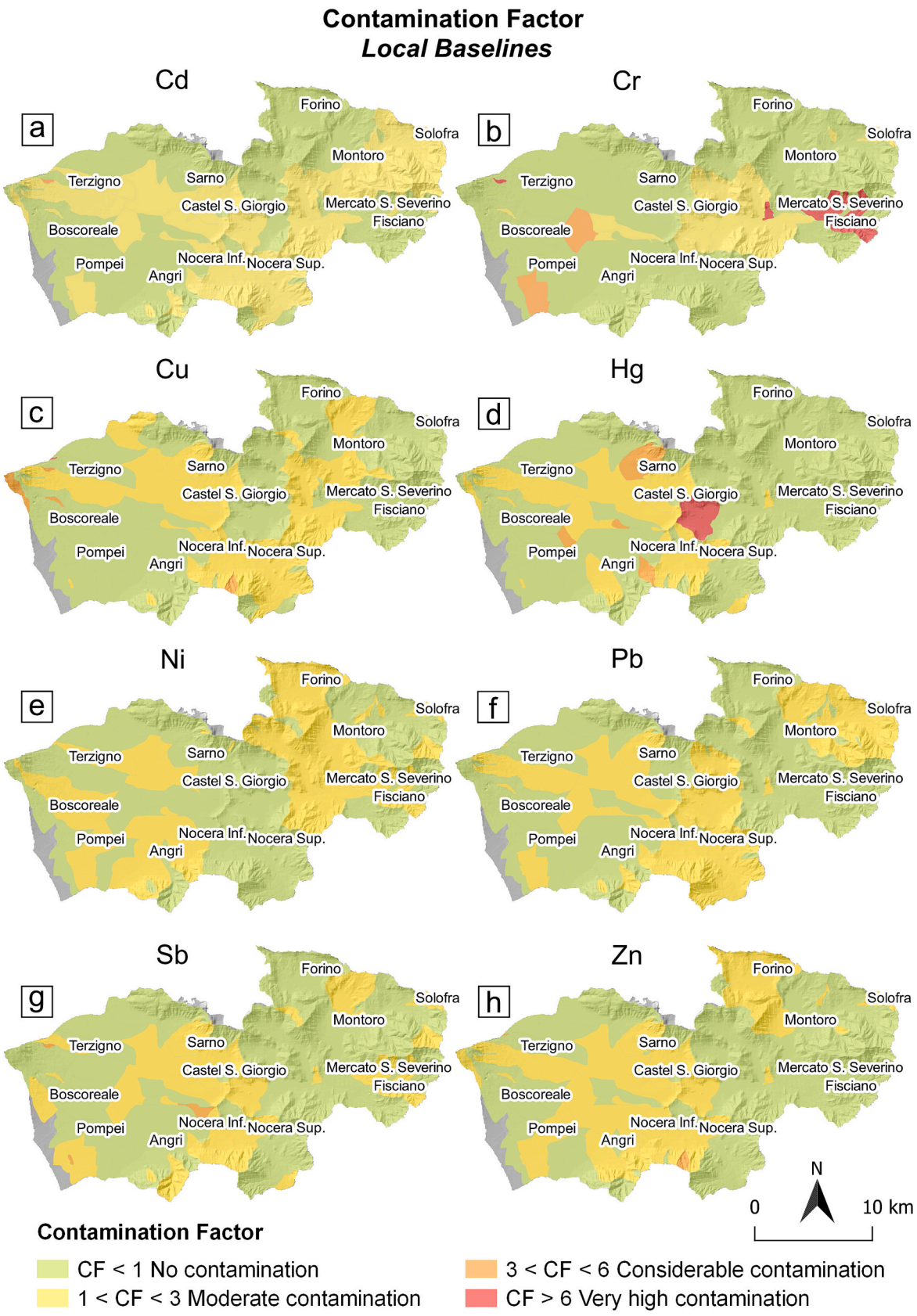

Fig. 4. Contamination Factor – Local Baselines (LBs) distribution maps for a) cadmium, b) chromium, c) copper, d) mercury, e) nickel, f) lead, g) antimony, h) zinc.

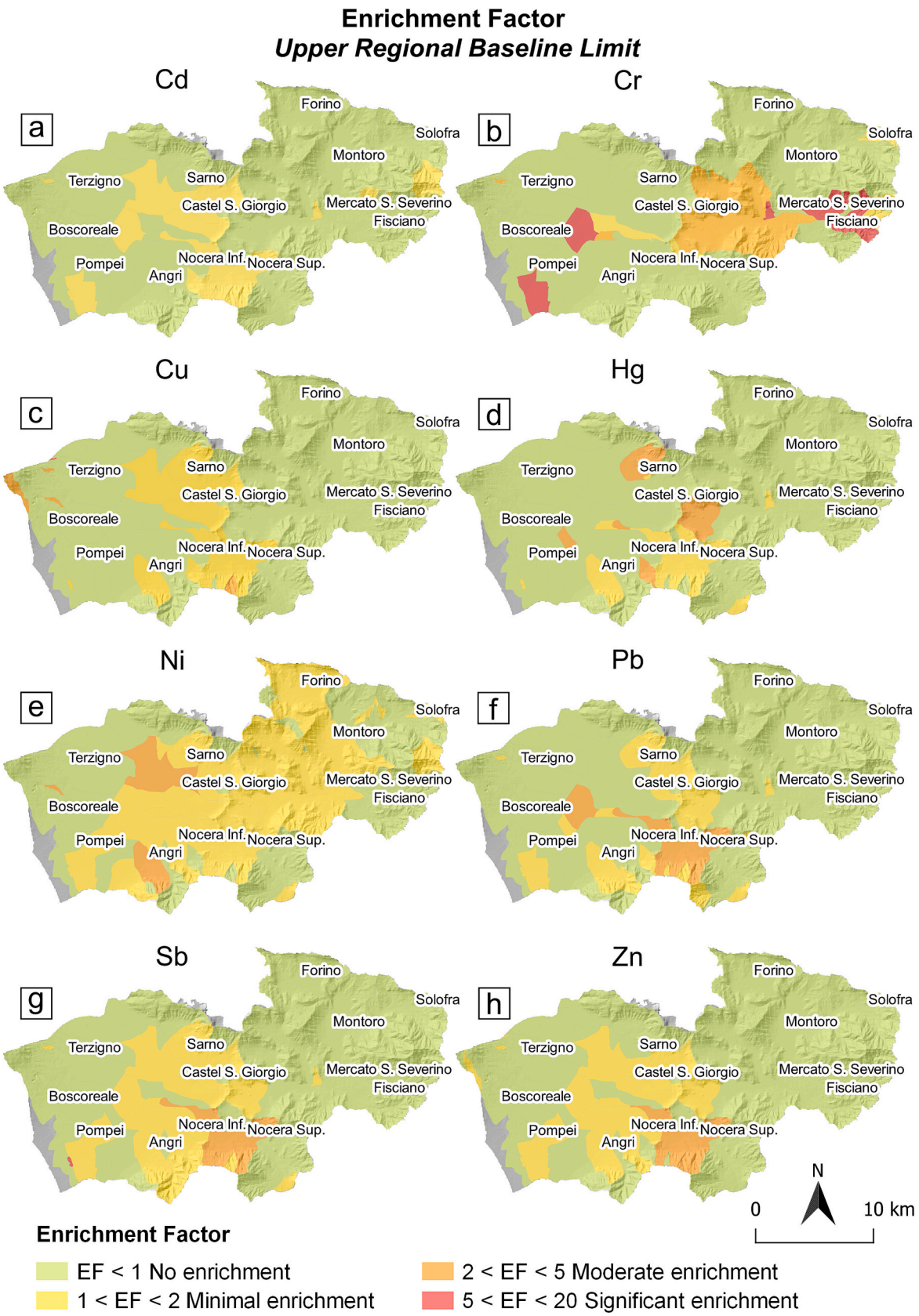

Fig. 5. Enrichment Factor – Upper Regional Baseline Limit distribution maps for a) cadmium, b) chromium, c) copper, d) mercury, e) nickel, f) lead, g) antimony, h) zinc.

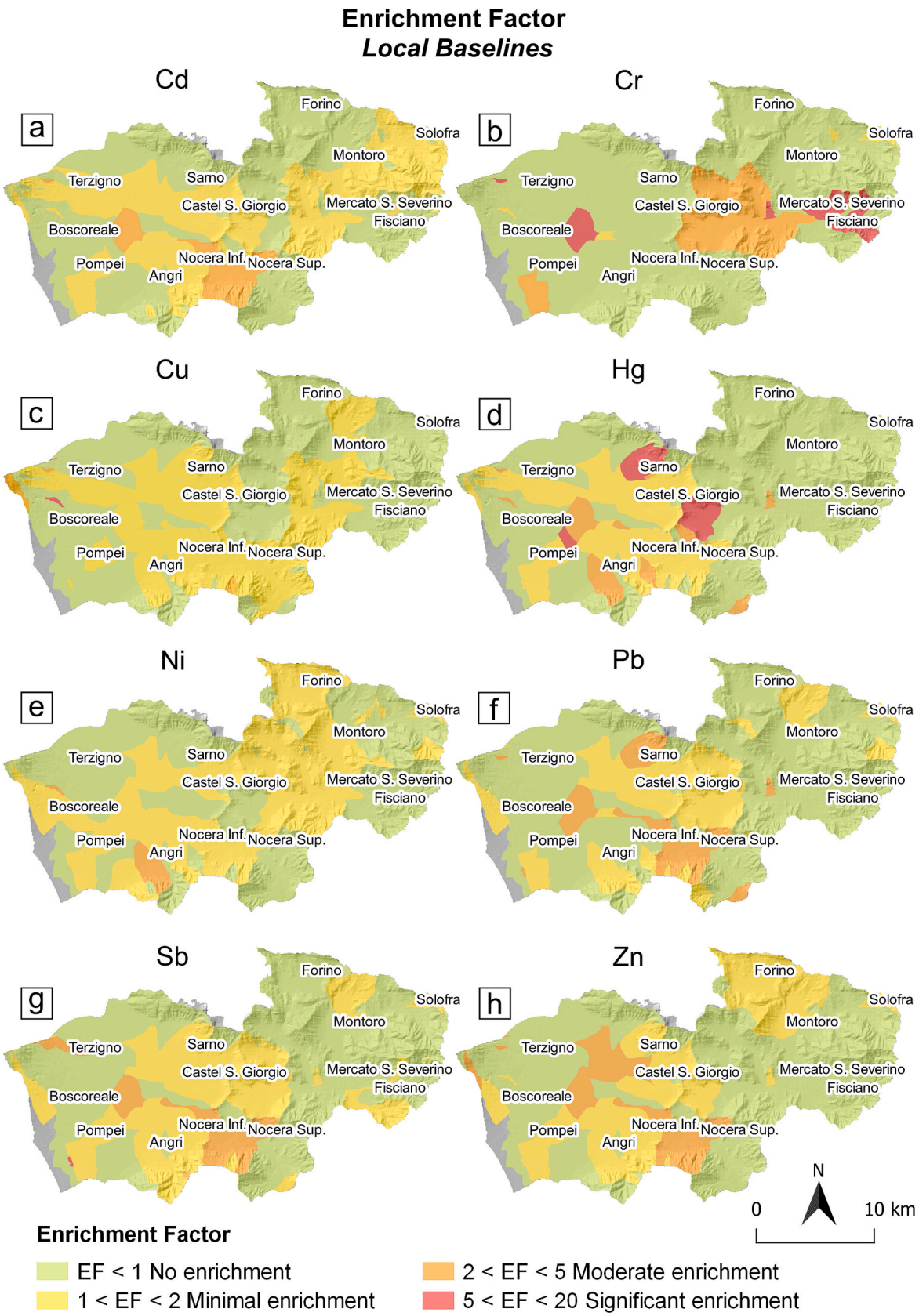

Fig. 6. Enrichment Factor – Local Baselines (LBs) distribution maps for a) cadmium, b) chromium, c) copper, d) mercury, e) nickel, f) lead, g) antimony, h) zinc.

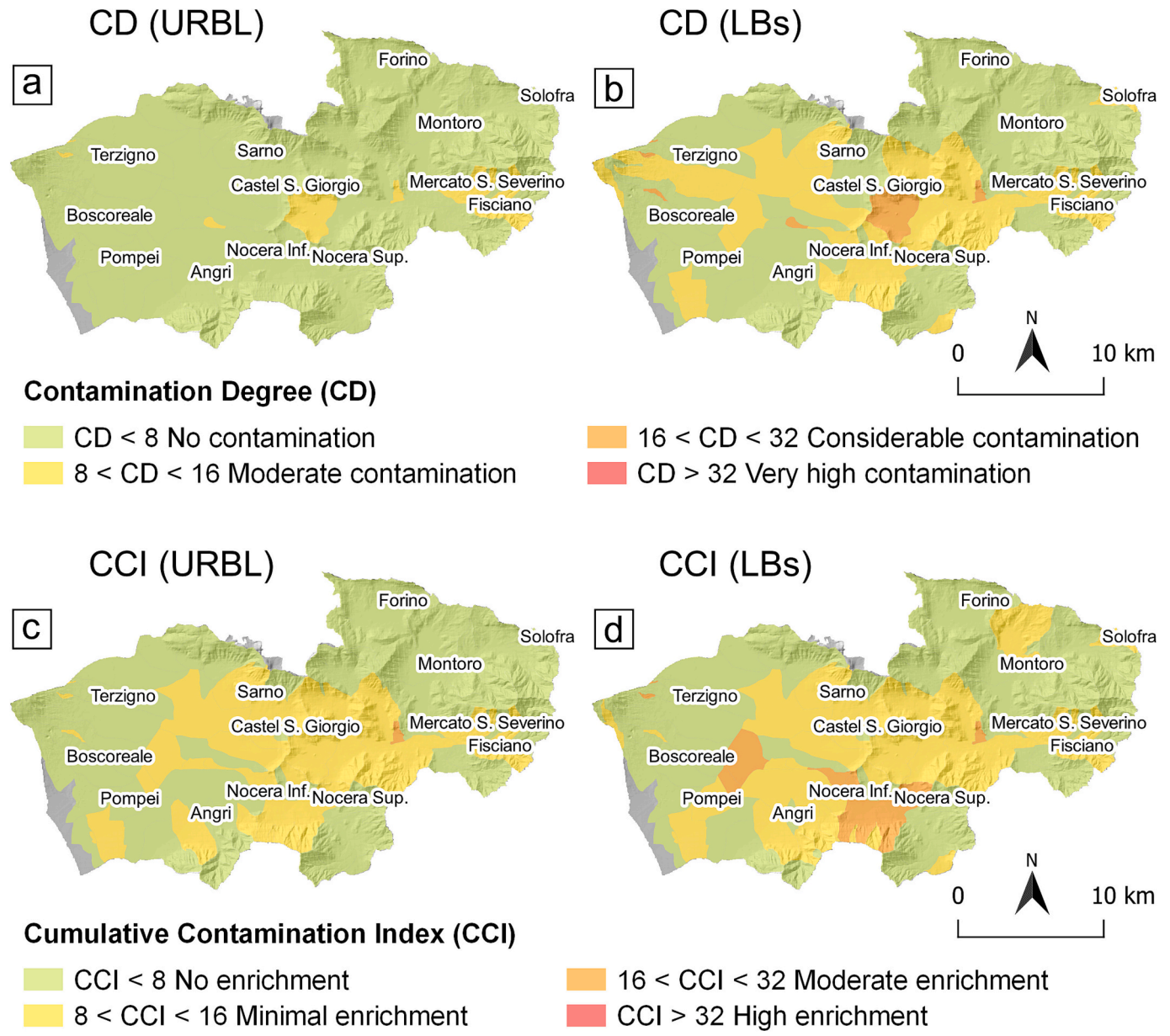

Fig. 7. Aggregated function distribution maps for a) Contamination Degree (CD) derived from URBL, b) Contamination Degree (CD) derived from LBs, c) Cumulative Contamination Index (CCI) derived from URBL, d) Cumulative Contamination Index (CCI) derived from LBs.

- CD > 28 Very high degree of contamination.

Similarly, CCI data were reclassified following the same approach:

- CCI < 7 No enrichment.
- 7 ≤ CCI ≤ 14 Minimal enrichment.
- 14 ≤ CCI ≤ 28 Moderate enrichment.
- CCI > 28 High enrichment.

4. Results

4.1. Contamination assessment for individual elements

4.1.1. Cadmium (Cd)

The URBL value for Cd was estimated as 0.88 mg/kg, whereas the average value of the LBs was estimated as 0.39 mg/kg (Table 2). The URBL value is located above the upper whisker (SM1).

Cadmium (Fig. 2a) shows the lowest baseline values (< 0.37 mg/kg), which characterise areas located in the northwest and northeast of the study area; medium values (0.37–0.44 mg/kg) are in the central part of the territory, and the highest values (> 0.44 mg/kg) characterised the

Table 2
Upper regional baseline limit (URBL) and Local Baselines (LBs, average value) of Cd, Cr, Cu, Hg, Ni, Pb, Sb, Zn and Fe. The significance of the Wilcoxon signed-rank test (*p*-value) is also reported (see discussion for more details).

Element	URBL	LBs (avg.)	Wilcoxon signed-rank (p-value)
Cd	0.88	0.39	< 0.001
Cr	139	97.1	< 0.001
Cu	263	116	< 0.001
Hg	489	143	< 0.001
Ni	24.9	17.5	< 0.001
Pb	146	67.3	< 0.001
Sb	1.82	0.82	< 0.001
Zn	404	153	< 0.001
Fe	40,945	26,588	< 0.001

areas toward the southwest. Considering the contamination indices calculated using URBL, the Cd-CF (Fig. 3a) values range between 0.1 and 1.3. The whole territory is characterised by CF values <1, indicating no contamination. Only one SCB presents a value between 1 and 3, indicating moderate contamination, in correspondence with the municipality of Terzigno. The Cd-EFs (Fig. 5a) range from 0.1 to 2.0 for raw data. Most of the study area presents EFs < 1, indicating no contamination. The highest values, between 1 and 2, indicate minimal enrichment and are located in the sector among the municipalities of Sarno and Nocera. Considering the contamination indices calculated by using LBs, the Cd-CF (Fig. 4a) values range from 0.2 to 3.3. Most of the study area presents no contamination, with CF values <1. Areas with moderate contamination, 1 < CF < 3, are distributed across the sector extending from the upstream zone, near the municipality of Solofra, to Terzigno, passing through Sarno, Nocera and Mercato San Severino municipalities. The Cd-EF (Fig. 6a) values range from 0.2 to 3.3. Most downstream sectors present EF values from 1 to >5, indicating high enrichment in areas such as Nocera. The remaining upstream sector, in correspondence with Forino's municipality, and part of the downstream area are characterised by no enrichment, with values <1.

4.1.2. Chromium (Cr)

The URBL value for Cr was estimated to be 139 mg/kg, whereas the average value of the LBs was estimated to be 97.1 mg/kg (Table 2). The URBL value is located between the 3rd quartile and the upper whisker (SM1). For Cr, the lowest local baseline values (< 98 mg/kg) (Fig. 2b) characterise those SCBs located in the north-east and north-west of the study area; medium values (98–121 mg/kg) are in the central part of the territory and the highest values (> 121 mg/kg) characterised areas toward the south-west. Considering the contamination indices calculated using URBL, the Cr-CF (Fig. 3b) values range from 0.03 to 8.0, with the most significant part of the territory characterised by values lower than 1, indicating no contamination. Areas with high contamination (CF > 6) correspond to the municipalities of Fisciano and Mercato S. Severino, turning into areas with moderate contamination (3 < CF < 6) as they proceed toward the downstream sectors. The Cr-EF (Fig. 5b) values range between 0.1 and 13.4. Most of the study area is characterised by EF < 1, indicating no enrichment. Areas with high or considerable contamination, EF > 2, are located along the river path spanning from the municipalities of Fisciano toward the area of Boscoreale. Considering contamination indices calculated using LBs, the CF (Fig. 4b) values range from 0.04 to 9.8. The spatial distribution of contamination values is similar to that estimated by URBL for Cr-CF; the only difference is the extension of the contamination plume in the downstream area between the Castel S. Giorgio and Boscoreale municipalities. The Cr-EFs (Fig. 6b) range between 0.03 and 10.2, and their spatial distribution follows the same behaviour as the Cr-EFs calculated using URBL.

4.1.3. Copper (Cu)

The URBL for Cu was estimated as 263 mg/kg, whereas the average value of LBs was estimated as 116 mg/kg (Table 2). The URBL value is located above the upper whisker (SM1). For Cu (Fig. 2c), the lowest local baseline values (< 98 mg/kg) characterised all the upstream area in the north-east sector; medium values (98–116 mg/kg) characterise the central part of the territory between the mountains chain and the plain, and the highest values (> 116 mg/kg) represent the whole downstream area. Considering the contamination indices calculated using URBL, the Cu-CF (Fig. 3c) values range from 0.1 to 5.1. Almost the totality of the study area is characterised by CFs < 1, indicating no contamination. Small areas with moderate to considerable contamination are present in the northwest and southern sectors of the territory, with CF values ranging from 1 to 6. The Cu-EFs (Fig. 5c) range between 0.2 and 6.7. Most of the study area presents EF values <1, indicating no enrichment; the highest values are in the central sector between the municipalities of Sarno, Nocera and Angri, indicating a moderate enrichment in Cu. Considering the contamination indices calculated using LBs, the Cu-CFs (Fig. 4c) range from 0.2 to 8.0. The most significant part of the territory presents CF values <1, while some areas are characterised by values between 3 and 6 in correspondence with the municipalities of Montoro, Mercato S. Severino, Nocera, Sarno, and Terzigno. The Cu-EF (Fig. 6c) values range from 0.3 to 8.1. Most of the territory is characterised by EFs between 1 and 2, indicating moderate enrichment, while EFs > 2, indicating significant enrichment, are primarily located in the northwest sector. The remaining areas are characterised by EFs < 1, indicating no enrichment.

4.1.4. Mercury (Hg)

The URBL value for Hg was 489 μg/kg, whereas the average value of the LBs was 143 μg/kg (Table 2). The URBL value is higher than the last outlier of the LBs (SM1). Mercury (Fig. 2d) shows the lowest baseline values (< 111 μg/kg), which characterise areas located in the northeast and northwest of the area; medium values (111–185 μg/kg) are in the central part of the territory, and the highest values (> 185 μg/kg) characterised the areas toward the southwest. Considering the contamination indices calculated using URBL, the Hg-CF values (Fig. 3d) range from 0.01 to 2.4. Most of the territory is characterised by CF values <1, indicating no contamination. Only two SCBs present values between 1 and 3, indicating moderate contamination, in correspondence with the municipalities of Sarno and Nocera. The Hg-EFs (Fig. 5d) range from 0.01 to 3.6 for raw data. Most of the study area presents EFs < 1, indicating no contamination. The highest values, between 2 and 5, indicate significant enrichment and are located in the sector among the municipalities of Sarno, Nocera, and Angri. Considering the contamination indices calculated using LBs, the Hg-CF values (Fig. 4d) range from 0.03 to 6.1. Most of the study area presents no contamination, with CF values <1. Areas with contamination from moderate to considerable, 1 < CF < 6, are in the downstream sector, with the highest values, CF > 6, located in the northern zone of the Nocera municipality. The Hg-EF (Fig. 6d) values range from 0.02 to 8.5. Most downstream sectors exhibit EF values ranging from 1 to >5, indicating high enrichment in areas such as Sarno and Nocera. The remaining downstream and the whole upstream sectors are characterised by no enrichment, with values <1.

4.1.5. Nickel (Ni)

The URBL value for Ni was estimated as 24.9 mg/kg, whereas the average value of the LBs was estimated as 17.5 mg/kg (Table 2). The URBL value is above the last outlier of the LBs (SM1). For Ni (Fig. 2e), the low baseline values (< 18 mg/kg) characterise the largest part of the territory, particularly the upstream areas, the northwest, and part of the central sector; the medium-high values (> 18 mg/kg) mark part of the downstream area and the sector among the municipalities of Forino and Mercato S. Severino. Considering the contamination indices calculated using URBL, the Ni-CF (Fig. 3e) values range from 0.3 to 1.8. Most of the study area presents CF < 1, indicating no contamination. The highest values, between 1 and 3, indicate moderate contamination and correspond to the municipalities of Montoro and Sarno. The Ni-EFs (Fig. 5e) values range from 0.5 to 2.3. Most of the territory presents EF values between 1 and 2, indicating minimal enrichment; the highest values, between 2 and 5, correspond with the municipalities of Sarno and Angri, indicating moderate enrichment. The remaining territory distinctly exhibits EFs < 1 for the northwest and upstream areas.

Considering the contamination indices calculated by using LBs, the Ni-CFs (Fig. 4e) range from 0.4 to 2.5. Part of the territory between the municipalities of Forino, Montoro, and Mercato S. Severino, as well as part of the downstream area between Sarno/Nocera and the coast, present CF values between 1 and 3, indicating moderate contamination. The remaining territory is characterised by no contamination, with CFs < 1. The Ni-EF (Fig. 6e) values range from 0.5 to 2.2. The spatial distribution is similar to that of the EFs calculated using the URBL, with most of the region exhibiting EF values ranging from 1 to 2, suggesting minimal enrichment. The municipality of Angri presents higher values,

ranging from 2 to 5, indicating moderate enrichment. In contrast, the rest of the territory shows EFs < 1, especially in the northwestern and upstream areas.

4.1.6. Lead (Pb)

The URBL value for Pb was estimated as 146 mg/kg, whereas the average value of the LBs is 67.3 mg/kg (Table 2). The URBL value is above the last outlier of the LBs (SM1). For Pb (Fig. 2f), the most significant part of the central areas from Fisciano to Sarno presents medium baseline values (61–75 mg/kg), with the last part of the downstream sector having the highest values (> 75 mg/kg). The lowest values (< 61 mg/kg) characterise the areas toward the northeast and northwest. Considering the contamination indices calculated using URBL, the Pb-CF values (Fig. 3f) range from 0.1 to 1.6. Almost the totality of the study area presents CF values <1, indicating no contamination. The highest values, between 1 and 3, indicating moderate contamination, are located in correspondence with the municipalities of Sarno, Nocera, and Mercato S. Severino. The Pb-EFs (Fig. 5f) range from 0.3 to 2.5. The central sector of the territory is characterised locally by EFs between 1 and 2, indicating a minimal enrichment; EF values between 2 and 5, indicating moderate enrichment, are located across the municipalities of Nocera and toward Pompei. The remaining territory is characterised by values <1, indicating no enrichment. Considering the contamination indices calculated using LBs, the Pb-CF values (Fig. 4f) range from 0.3 to 2.9. The highest CF values, between 1 and 3, indicating moderate contamination, are in the upstream sector and the area spanning from the municipalities of Castel S. Giorgio and Nocera to Terzigno. The remaining territory is characterised by no contamination, with CFs < 1. The Pb-EFs (Fig. 6f) range from 0.3 to 3.4. The central sector of the territory is characterised by EFs between 1 and 2, indicating minimal enrichment; values between 2 and 5, indicating moderate enrichment, are located across the municipalities of Nocera, Sarno, and Pompei. The remaining territory is characterised by values <1, indicating no enrichment.

4.1.7. Antimony (Sb)

The URBL value for Sb was estimated as 1.82 mg/kg, whereas the average value of the LBs was estimated as 0.82 mg/kg (Table 2). The URBL value is above the last outlier of the LBs (SM1). The Sb (Fig. 2g) shows the intermediate baseline values (< 0.7 mg/kg) characterising the central part of the territory; the lowest values (< 0.7 mg/kg) mark the areas along the northern sector, and the highest values are (> 1.0 mg/kg) in correspondence of the municipalities of Nocera, Angri and Pompei. Considering the contamination indices calculated using URBL, the Sb-CF values (Fig. 3g) range from 0.2 to 2.7. Almost the totality of the study area presents no contamination, with CFs < 1, except for the area across the municipality of Nocera, which is characterised by moderate contamination, with values between 1 and 3. The Sb-EFs (Fig. 5g) range from 0.2 to 5.6. The values between 1 and 2, indicating a minimal enrichment, characterise most of the central sector, with the highest values, between 2 and 5, in correspondence with the Nocera municipality. The remaining territory presents no enrichment, with EFs < 1. Considering the contamination indices calculated using LBs, the Sb-CF values (Fig. 4g) range from 0.2 to 4.4. Most of the study area is characterised by CFs < 1, indicating no contamination. Values between 1 and 3, indicating moderate contamination, are distributed locally in the territory, particularly in the central region. The highest values, CF > 3, indicating considerable contamination, are located across the municipalities of Nocera and Terzigno. The Sb-EF (Fig. 6g) values range from 0.2 to 5.4. The spatial distribution is very similar to the Sb-EFs calculated by URBL; additionally, some central areas close to the Terzigno and Angri municipalities exhibit EFs between 2 and 5, indicating moderate enrichment.

4.1.8. Zinc (Zn)

The URBL value for Zn was estimated to be 404 mg/kg, whereas the average value of the LBs was estimated to be 153 mg/kg (Table 2). The URBL value is located above the last outlier of LBs. For Zn (Fig. 2h), the medium baseline values (121–189 mg/kg) characterise the majority of the area, with the highest values (>189 mg/kg) located in the downstream sector. The lowest values tend to mark the areas in correspondence with the Solofra, Boscoreale and Terzigno municipalities. Considering the contamination indices calculated using URBL, the Zn-CF values (Fig. 3h) range from 0.1 to 1.3. Almost the totality of the study area presents no contamination, with CF values <1, except for the territory between the municipalities of Sarno and Nocera, which shows values between 1 and 3, indicating moderate contamination. The Zn-EFs (Fig. 5h) range from 0.2 to 2.6. Most of the study area is characterised by no enrichment. EF values between 1 and 2 describe most of the downstream sector, with the highest values, between 2 and 5, located across the Nocera municipality. Considering the contamination indices calculated using LBs, the Zn-CF values (Fig. 4h) range between 0.2 and 3.1. The CFs between 1 and 3, indicating moderate contamination, are in the northeast and most downstream sectors. The remaining territory is characterised by no contamination, with CFs < 1. The Zn-EFs (Fig. 6g) values range between 0.2 and 3.6. Significant parts of the downstream sector, particularly areas across the municipalities of Forino and Montoro, are characterised by values between 1 and 2. The areas between Sarno and Nocera exhibit moderate enrichment, with values ranging from 2 to 5. The remaining territory presents no enrichment, with EFs < 1.

4.2. Aggregate contamination assessment

4.2.1. Contamination Degree (CD)

Using the URBL values, the CD values (Fig. 7a) range from 0.9 to 12.1. Almost all the territory is characterised by no contamination, with CD < 8; the highest values range between 7 and 14, indicating moderate contamination, and are located across the municipalities of Fisciano and Nocera. Considering the LBs, the CD values (Fig. 7b) range from 2.0 to 23.8. Most of the territory is characterised by CD < 8; the central sector and some areas between Sarno and Pompei municipalities are marked by the most part of the territory is characterised by CD < 8; central sector and some areas between Sarno and Pompei municipalities are marked by moderate contamination, with values from 8 to 16. The highest values, ranging from 16 to 32, indicating high contamination, are locally concentrated between the municipalities of Fisciano and Nocera.

4.2.2. Cumulative contamination index (CCI)

Using the URBL values, the CCI values (Fig. 7c) range from 1.8 to 20.7. The lowest values, CCI < 8, are found in the upstream and northwest sectors of the study area; values indicating minimal enrichment, 8 < CCI < 16, are identified in most areas of the central and downstream sectors. The highest value, 16 < CCI < 32, indicating moderate enrichment, is locally distributed in correspondence with the municipalities of Mercato S. Severino and Castel S. Giorgio. Otherwise, using the LBs, CCI values (Fig. 7d) range between 1.5 and 23.9. The spatial distribution is similar to the CCI calculated using the URBL, with the lowest and medium values located in the upstream and central/downstream sectors, respectively. One of the detectable differences regards high values, 16 < CCI < 32, which majorly characterise some areas between the municipalities of Sarno, Nocera and Pompei.

5. Discussion

The primary objective of this study was to establish geochemical baselines for assessing contamination in stream sediment samples, employing two distinct methodologies.

A one-sample *t*-test was carried out to compare the URBL values with the average value of the LBs, evaluating the distinction between the two baseline methods. Specifically, the Wilcoxon signed-rank test is a non-

parametric test used to compare the mean of a group (LBs) with a reference mean (URBL value), assuming that the data are not normally distributed, as is the case in this work. The resulting p-value <0.001 indicates that the observed difference between the two compared values is unlikely to be due to random chance alone; therefore, there is a statistically significant difference between the use of URBL and LBs.

Comparing the results from the unique baseline and local baseline approaches showed significant differences in assessing contamination levels. The URBL approach provided a wider view, highlighting overall contamination trends across the area. In contrast, the LBs approach provided a more detailed perspective, capturing variations influenced by local geology and land-use practices. This behaviour is also reflected in the distribution maps of contamination indices. The CFs and EFs calculated by the LBs tend to enhance the signal in moderately and heavily contaminated areas, especially in the downstream sectors, and in correspondence with the municipalities of Castel S. Giorgio and Mercato S. Severino, where the intense anthropogenic pressure in these areas is well known. This is particularly true for the CFs, which appear to be more responsive to the implementation of the local baselines, exhibiting a general enhancement for all elements (Figs. 3 and 4). Regarding the EFs, elements such as Hg, Pb, Zn, Cd and Cu exhibit a more pronounced enhancement than the others (Figs. 5 and 6). This enhancement would allow a better discrimination of those urban and industrial areas which are historically characterised by anthropogenic pressure deriving from traffic vehicles (Pb, Cd, Sb), ceramics (Pb, Cd), furniture factories (Ni, Sb), tanneries (Cr, Hg, Ni) as well as agricultural practices (Cd, Cu, Zn) (Albanese et al., 2013; Cicchella et al., 2014).

Regarding aggregated functions maps (Fig. 7), the Contamination Degree (CD) calculated using the local baseline exhibits a significant change, strongly emphasising the moderately to considerably contaminated areas near Castel San Giorgio and Mercato San Severino municipalities. Similarly, the Cumulative Contamination Index (CCI) highlights an intensified signal in some downstream areas near Sarno and Nocera, shifting from minimal to moderate enrichment. However, the maps clearly indicate that the usage of local baselines is more effective for the Contamination Degree (CD) than for the CCI. This is likely due to the Enrichment Factor (EF)'s higher stability than the Contamination Factor (CF), as EF normalises the data using a reference value, thereby compensating for natural variations.

A comparison of the boxplots (Fig. 8a and b) between the aggregate functions calculated using both methods shows that the CD and CCI values derived from LBs have a wider value range, allowing a better subdivision of values. This is also evident in the kernel density distribution (Fig. 8c and d), where the CD and CCI curves derived from LBs result in smoothed peaks and tend to extend their range of values. However, to quantitatively describe the improvement achieved by using LBs, a threshold-based classification approach was applied to both the URBL and LB data. For each aggregate function, the number of SCBs exceeding the contamination threshold ($CD > 8$; $CCI > 8$) was counted in both scenarios. The relative improvement was then calculated using the following equation:

$$Percentage\ Increase = \frac{N_{LBs} - N_{URBL}}{N_{URBL}} \quad (9)$$

where N_{LBs} and N_{URBL} represent the number of SCBs identified as contaminated ($CD > 8$; $CCI > 8$) using LBs and URBL, respectively. Based on this approach, the CCI (based on the sum of EFs) showed a 23 % increase in the detection of contaminated sub-basins. In comparison, the CD (based on the sum of CFs) exhibited a 366 % increase, which is approximately four times higher than the index calculated by the URBL.

Additionally, to quantitatively evaluate the improvement introduced by SCB-corrected data and LBs, a dedicated sensitivity analysis was performed to quantify the contribution of each element to the respective aggregate function. Ideally, each variable should contribute equally, meaning the total variance of the aggregate function (100 %) should be evenly distributed among all variables. In our case, each variable should contribute approximately 14 % (100 % /number of variables) to the aggregate function for a uniform distribution. This is done by calculating the correlation of each independent variable (CF/EF of single element) with respect to the dependent variable (CD/CCI). The squared correlation coefficient determined the contribution of each variable to the total variance. The variables were then ranked according to their contribution (Fig. 8e and f). The SCB-corrected data appear to have stabilised the variations in the weights of individual elements, particularly those with higher significant variations (Cu, Cr, Pb), which show a rebalancing of their concentrations. The resulting weights indicate that the element concentrations have been corrected to better reflect the actual contamination, reducing the predominance of some elements and increasing the significance of others. This leads to a more accurate overall assessment and is less prone to distortions due to high concentrations of a few elements. This is particularly clear with CFs rather than EFs, as they have been subjected to less weight redistribution. This is probably because the EF is more stable than the CF, as it normalises element concentration relative to a stable and abundant reference element.

Since this is the first application of the SCB method to the calculation of contamination indices, it is not possible to make a direct comparison with other case studies. Nevertheless, it is worth noting that while the use of a unique reference background (URBL) is a widely adopted and practical starting point for contamination assessment (particularly when global or regional geochemical values are used (Kalita et al., 2019; Varol et al., 2020; Wang et al., 2025), this approach may overlook local-scale lithological variability. As demonstrated in this study, integrating local baseline values allows for a more accurate and spatially sensitive evaluation of contamination, better reflecting the actual local environmental conditions of the study area. In this sense, the proposed method represents a methodological advancement, as it reduces the risk of over- or underestimating contamination levels due to generalized geochemical references. In fact, by referring to the work of Albanese et al. (2013) on the Sarno River basin, it can be observed that the results obtained do not alter the overall view of contamination, where polluted areas are mainly concentrated in the central and downstream sectors. However, the first application of the local baseline to the contamination indices provides a more detailed representation of the contamination framework. This is further supported by the sensitivity analysis, which confirms that the individual indices contribute with major equilibrium to the value of the aggregate functions.

Further, while the Sarno River basin served as a case study, the proposed approach has broader relevance and can be applied to other fluvial systems. This is primarily due to its limited input requirements, which include a digital elevation model (DEM) to derive hydrological and morphological features, and a set of sampling points acting as hydrological outlets for delineating each sub-basin. These inputs are often available from the main open-source spatial databases, making the approach accessible and adaptable. Additionally, while the inclusion of further geochemical elements is possible, it depends on the availability of relevant geochemical data. The level of detail, however, depends on the sampling density. Nevertheless, even with a relatively low number of samples, this method provides a more spatially accurate understanding.

6. Conclusions

This study investigates the development of a method that accounts for the spatial variability of baseline values within a river catchment, considering both geological variations in the substrate and the dynamic nature of transported sediments. The results indicate that the use of SCB-based baseline values led to a 26 % increase in the detection of highly contaminated sites using the Enrichment Factor and a 366 % increase using the Contamination Factor, revealing a substantial underestimation of contamination in the traditional URBL approach. Moreover, the sensitivity analysis of contamination indices revealed that the

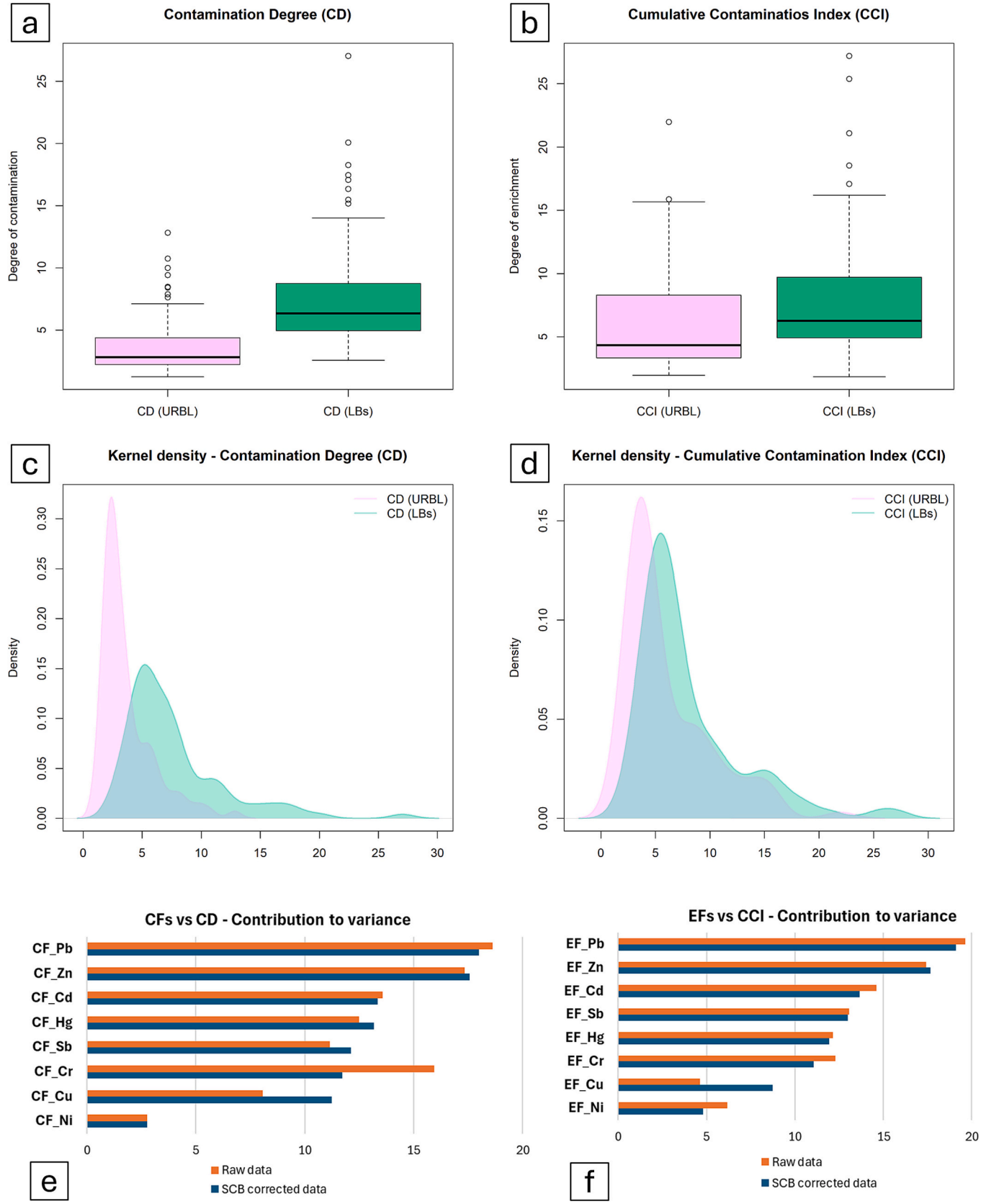

Fig. 8. a) comparison between Contamination Degree values derived from URBL and LBs; b) comparison between Cumulative Contamination Index values derived from URBL and LBs; c) kernel density distribution for Contamination degree derived by using URBL and LBs; d) kernel density distribution for Cumulative Contamination Index derived by using URBL and LBs; e) sensitivity analysis for CD; f) sensitivity analysis for CCI.

traditional approach can create imbalances in the contributions of different variables. In contrast, the SCB approach, using LBs, provides a more homogeneous weighting, suggesting that balancing each variable's contribution enhances the performance of contamination assessment functions. This leads to a more accurate and spatially representative evaluation of environmental quality. Overall, the SCB-based approach can significantly enhance the reliability and applicability of contamination assessment, providing a scalable tool for environmental monitoring in heterogeneous basins, where a uniform baseline approach may lead to misinterpretation or underestimation of contamination levels.

Supplementary data to this article can be found online at https://doi.org/10.1016/j.gexplo.2025.107860.

CRediT authorship contribution statement

Iannone Antonio: Writing – original draft, Software, Methodology, Investigation, Formal analysis, Data curation, Conceptualization. **Dominech Salvatore:** Writing – original draft, Validation, Methodology. **Pacifico Lucia Rita:** Validation. **Guarino Annalise:** Validation. **Albanese Stefano:** Writing – original draft, Supervision, Resources, Funding acquisition, Conceptualization.

Declaration of competing interest

The authors declare that they have no known competing financial interests or personal relationships that could have appeared to influence the work reported in this paper.

Acknowledgments

This study was carried out within the RETURN Extended Partnership and received funding from the European Union NextGenerationEU (National Recovery and Resilience Plan (NRRP), Mission 4, Component 2, Investment 1.3—D.D. 1243 2/8/2022, PE0000005).

Data availability

Data will be made available on request.

References

Albanese, S., Iavazzo, P., Adamo, P., Lima, A., De Vivo, B., 2013. Assessment of the environmental conditions of the Sarno river basin (south Italy): a stream sediment approach. Environ. Geochem. Health 35, 283–297. https://doi.org/10.1007/s10653-012-9483-x.

Arienzo, M., Adamo, P., Rosaria Bianco, M., Violante, P., 2001. Impact of land use and urban runoff on the contamination of the Sarno river basin in southwestern Italy. Water Air Soil Pollut. 131, 349–366. https://doi.org/10.1023/A:1011908019933.

Aruta, A., Albanese, S., Daniele, L., Cannatelli, C., Buscher, J.T., De Vivo, B., Petrik, A., Cicchella, D., Lima, A., 2023. A new approach to assess the degree of contamination and determine sources and risks related to PTEs in an urban environment: the case study of Santiago (Chile). Environ. Geochem. Health 45, 275–297. https://doi.org/10.1007/s10653-021-01185-6.

Barbieri, M., 2016. The importance of enrichment factor (EF) and geoaccumulation index (Igeo) to evaluate the soil contamination. J. Geol. Geophys. 5. https://doi.org/10.4172/2381-8719.1000237.

Bonham-Carter, G.F., Rogers, P.J., Ellwood, D.J., 1987. Catchment basin analysis applied to surficial geochemical data, Cobequid Highlands, Nova Scotia. J. Geochem. Explor. 29, 259–278. https://doi.org/10.1016/0375-6742(87)90081-1.

Califano, F., Mobilia, M., Longobardi, A., 2015. Heavy rainfall temporal characterization in the peri-urban solofrana River Basin, Southern Italy. Procedia Eng 119, 1129–1138. https://doi.org/10.1016/j.proeng.2015.08.957.

Carranza, E.J.M., 2009. Chapter 5: catchment basin analysis of stream sediment anomalies. In: Carranza, E.J.M. (Ed.), Handbook of Exploration and Environmental Geochemistry. Elsevier Science B.V., pp. 115–144. https://doi.org/10.1016/S1874-2734(09)70009-9

Carranza, E.J.M., 2011. Analysis and mapping of geochemical anomalies using logratio-transformed stream sediment data with censored values. J. Geochem. Explor. 110, 167–185. https://doi.org/10.1016/j.gexplo.2011.05.007.

Carranza, Emmanuel John M., Hale, M., 1997. A catchment basin approach to the analysis of reconnaissance geochemical-geological data from Albay Province, Philippines. J. Geochem. Explor. 60, 157–171. https://doi.org/10.1016/S0375-6742(97)00032-0.

Carrillo, K.C., Drouet, J.C., Rodríguez-Romero, A., Tovar-Sánchez, A., Ruiz-Gutiérrez, G., Viguri Fuente, J.R., 2021. Spatial distribution and level of contamination of potentially toxic elements in sediments and soils of a biological reserve wetland, northern Amazon region of Ecuador. J. Environ. Manage. 289, 112495. https://doi.org/10.1016/j.jenvman.2021.112495.

Cheng, J., Shi, Z., Zhu, Y., 2007. Assessment and mapping of environmental quality in agricultural soils of Zhejiang Province, China. J. Environ. Sci. 19, 50–54. https://doi.org/10.1016/S1001-0742(07)60008-4.

Cicchella, D., Giaccio, L., Lima, A., Albanese, S., Cosenza, A., Civitillo, D., De Vivo, B., 2014. Assessment of the topsoil heavy metals pollution in the Sarno River basin, south Italy. Environ. Earth Sci. 71, 5129–5143. https://doi.org/10.1007/s12665-013-2916-8.

Cinque, A., Aucelli, P., Brancaccio, L., Mele, R., Milia, A., Robustelli, G., Romano, P., Russo, F., Russo, M., Santangelo, N., Sgambati, D., 1997. Volcanism, tectonics and recent geomorphological change in the Bay of Napoli. Suppl. Geogr. Fis. Dinam. Quat. 3, 123–141.

De Pippo, T., Donadio, C., Guida, M., Petrosino, C., 2006. The Case of Sarno River (Southern Italy). Effects of geomorphology on the environmental impacts (8 pp). Environ. Sci. Pollut. Res. 13, 184–191. https://doi.org/10.1065/espr2005.08.287.

Dominech, S., Yang, S., Aruta, A., Gramazio, A., Albanese, S., 2022. Multivariate analysis of dilution-corrected residuals to improve the interpretation of geochemical anomalies and determine their potential sources: the Mingardo River case study (Southern Italy). J. Geochem. Explor. 232, 106890. https://doi.org/10.1016/j.gexplo.2021.106890.

EEA, 2018. Corine land cover (CLC), Copernicus Land monitoring service [WWW Document]. Corine Land Cover. https://doi.org/10.2909/71c95a07-e296-44fc-b22b-415f42acfdf0.

Ergin, M., Saydam, C., Baştürk, Ö., Erdem, E., Yörük, R., 1991. Heavy metal concentrations in surface sediments from the two coastal inlets (Golden Horn Estuary and İzmit Bay) of the northeastern Sea of Marmara. Chem. Geol. 91, 269–285. https://doi.org/10.1016/0009-2541(91)90004-B.

Habibnia, A., Rahimipour, Gh.R., Ranjbar, H., 2019. Anomaly delineation of porphyry copper deposits of Hanza Region through geochemical data analyses and multispectral remote sensing. J. Min. Environ. 10, 747–762. https://doi.org/10.22044/jme.2019.8203.1695.

Hakanson, L., 1980. An ecological risk index for aquatic pollution control.a sedimentological approach. Water Res. 14, 975–1001. https://doi.org/10.1016/0043-1354(80)90143-8.

Haris, H., Looi, L.J., Aris, A.Z., Mokhtar, N.F., Ayob, N.A.A., Yusoff, F.Md., Salleh, A.B., Praveena, S.M., 2017. Geo-accumulation index and contamination factors of heavy metals (Zn and Pb) in urban river sediment. Environ. Geochem. Health 39, 1259–1271. https://doi.org/10.1007/s10653-017-9971-0.

He, Z., Li, F., Dominech, S., Wen, X., Yang, S., 2019. Heavy metals of surface sediments in the Changjiang (Yangtze River) Estuary: distribution, speciation and environmental risks. J. Geochem. Explor. 198, 18–28. https://doi.org/10.1016/j.gexplo.2018.12.015.

Ip, C.C.M., Li, X.D., Zhang, G., Wong, C.S.C., Zhang, W.L., 2005. Heavy metal and Pb isotopic compositions of aquatic organisms in the Pearl River Estuary, South China. Environ. Pollut. 138, 494–504. https://doi.org/10.1016/J.ENVPOL.2005.04.016.

Johnson, T., Butcher, J., Santell, S., Schwartz, S., Julius, S., LeDuc, S., 2022. A review of climate change effects on practices for mitigating water quality impacts. J. Water Clim. Chang. 13 (4), 1684–1705. https://doi.org/10.2166/wcc.2022.363.

Kadhum, S.A., et al., 2015. Evaluation of the status and distributions of heavy metal pollution in surface sediments of the Langat River Basin in Selangor Malaysia. Mar. Pollut. Bull. 101 (1), 391–396. Available at: https://doi.org/10.1016/j.marpolbul.2015.10.012.

Kalita, S., Sarma, H.P., Devi, A., 2019. Sediment characterisation and spatial distribution of heavy metals in the sediment of a tropical freshwater wetland of Indo-Burmese province. Environ. Pollut. 250, 969–980. https://doi.org/10.1016/j.envpol.2019.04.112.

Kowalska, J.B., Mazurek, R., Gąsiorek, M., Zaleski, T., 2018. Pollution indices as useful tools for the comprehensive evaluation of the degree of soil contamination–a review. Environ. Geochem. Health 40, 2395–2420. https://doi.org/10.1007/s10653-018-0106-z.

Lancianese, V., Dinelli, E., 2015. Different spatial methods in regional geochemical mapping at high density sampling: An application on stream sediment of Romagna Apennines, Northern Italy. J. Geochem. Explor. 154, 143–155. https://doi.org/10.1016/j.gexplo.2014.12.014.

Longobardi, A., Diodato, N., Mobilia, M., 2016. Historical storminess and hydro-geological hazard temporal evolution in the Solofrana River Basin—Southern Italy. Water (Basel) 8, 398. https://doi.org/10.3390/w8090398.

Loska, K., Cebula, J., Pelczar, J., Wiechuła, D., Kwapuliński, J., 1997. Use of enrichment, and contamination factors together with geoaccumulation indexes to evaluate the content of Cd, Cu, and Ni in the Rybnik water reservoir in Poland. Water Air Soil Pollut. 93, 347–365. https://doi.org/10.1023/A:1022121615949.

Luo, Y., Wang, N., Liu, Z., Sun, Y., Lu, N., 2024. Characteristics and risk assessment of potentially toxic elements pollution in river water and sediment in typical gold mining areas of Northwest China. Sci. Rep. 14, 12715. https://doi.org/10.1038/s41598-024-63723-3.

Matschullat, J., Ottenstein, R., Reimann, C., 2000. Geochemical background – can we calculate it? Environ. Geol. 39, 990–1000. https://doi.org/10.1007/s002549900084.

Montuori, P., Lama, P., Aurino, S., Naviglio, D., Triassi, M., 2013. Metals loads into the Mediterranean Sea: estimate of Sarno River inputs and ecological risk. Ecotoxicology 22, 295–307. https://doi.org/10.1007/s10646-012-1026-9.

Montuori, P., Aurino, S., Nardone, A., Cirillo, T., Triassi, M., 2015. Spatial distribution and partitioning of organophosphates pesticide in water and sediment from Sarno River and Estuary, Southern Italy. Environ. Sci. Pollut. Res. 22, 8629–8642. https://doi.org/10.1007/s11356-014-4016-z.

Muller, G., 1969. Index of geoaccumulation in sediments of the Rhine River. GeoJournal 2, 108–118.

Najafian, T., Mokhtari, A.R., Albanese, S., 2020. 3D analysis of catchment basins by incorporating modified dilution correction equations in geochemical anomaly delineation. J. Geochem. Explor. 216, 106574. https://doi.org/10.1016/j.gexplo.2020.106574.

Niu, S., Wang, R., Jiang, Y., 2024. Quantification of heavy metal contamination and source in urban water sediments using a statistically determined geochemical baseline. Environ. Res. 263, 120080. https://doi.org/10.1016/j.envres.2024.120080.

Pejman, A., Nabi Bidhendi, G., Ardestani, M., Saeedi, M., Baghvand, A., 2015. A new index for assessing heavy metals contamination in sediments: a case study. Ecol. Indic. 58, 365–373. https://doi.org/10.1016/j.ecolind.2015.06.012.

Pepi, M., Borra, M., Tamburrino, S., Saggiomo, M., Viola, A., Biffali, E., Balestra, C., Sprovieri, M., Casotti, R., 2016. A Bacillus sp. isolated from sediments of the Sarno River mouth, Gulf of Naples (Italy) produces a biofilm biosorbing Pb(II). Sci. Total Environ. 562, 588–595. https://doi.org/10.1016/j.scitotenv.2016.04.097.

Reimann, C., Filzmoser, P., Garrett, R.G., 2005. Background and threshold: critical comparison of methods of determination. Sci. Total Environ. 346, 1–16. https://doi.org/10.1016/j.scitotenv.2004.11.023.

Reimann, C., Filzmoser, P., Garrett, R.G., Dutter, R., 2008. Statistical Data Analysis Explained, Journal of Physics A: Mathematical and Theoretical. John Wiley & Sons, Ltd, Chichester, UK. https://doi.org/10.1002/9780470987605.

Rolandi, G., Paone, A., Di Lascio, M., Stefani, G., 2008. The 79 AD eruption of Somma: The relationship between the date of the eruption and the southeast tephra dispersion. J. Volcanol. Geotherm. Res. 169, 87–98. https://doi.org/10.1016/j.jvolgeores.2007.08.020.

Salminen, R., 1995. Regional Geochemical Mapping in Finland in 1982-1994, p. 130.

Tarquini, S., Isola, I., Favalli, M., Battistini, A., Dotta, G., 2023. TINITALY, a digital elevation model of Italy with a 10 meters cell size (Version 1.1). Istituto Nazionale di Geofisica e Vulcanologia (INGV). https://doi.org/10.13127/tinitaly/1.1.

Tomlinson, D., Wilson, J., Harris, C.R., Jeffrey, D.W., 1980. Problems in assessment of heavy metals in estuaries and the formation of pollution index. Helgoländer Meeresuntersuchungen 33, 566–575. https://doi.org/10.1007/BF02414780.

Varol, M., 2011. Assessment of heavy metal contamination in sediments of the Tigris River (Turkey) using pollution indices and multivariate statistical techniques. J. Hazard. Mater. 195, 355–364. Available at: https://doi.org/10.1016/j.jhazmat.2011.08.051.

Varol, M., Sünbül, M.R., Aytop, H., Yılmaz, C.H., 2020. Environmental, ecological and health risks of trace elements, and their sources in soils of Harran Plain, Turkey. Chemosphere 245, 125592. https://doi.org/10.1016/j.chemosphere.2019.125592.

Vineethkumar, V., Sayooj, V.V., Shimod, K.P., Prakash, V., 2020. Estimation of pollution indices and hazard evaluation from trace elements concentration in coastal sediments of Kerala, Southwest Coast of India. Bull. Natl. Res. Cent. 44, 198. https://doi.org/10.1186/s42269-020-00455-0.

Wang, W., Wang, S., Chen, J., Jiang, X., Zheng, B., 2019. Combined use of diffusive gradients in thin film, high-resolution dialysis technique and traditional methods to assess pollution and bioavailability of sediment metals of lake wetlands in Taihu Lake Basin. Sci. Total Environ. 671, 28–40. https://doi.org/10.1016/j.scitotenv.2019.03.053.

Wang, J., Tao, L., Ren, H., Xue, X., Yang, Z., Jiang, Y., Ren, J., 2025. Assessment of surface sediment properties and heavy metal contamination in typical urban areas of the Yellow River, China. Sci Rep 15, 9403. https://doi.org/10.1038/s41598-025-87503-9.